Available online at www.sciencedirect.com
ScienceDirect
Ceramics International 38 (2012) 341–349
CERAMICS INTERNATIONAL
www.elsevier.com/locate/ceramint

A porous hydroxyapatite scaffold for bone tissue engineering: Physico-mechanical and biological evaluations

Garima Tripathi, Bikramjit Basu *

Laboratory for Biomaterials Department of Material Science and Engineering Indian Institute of Technology, Kanpur 208016, U.P., India

Received 7 May 2011; accepted 5 July 2011
Available online 18th July 2011

Abstract

Polymer sponge replication method was used in this study to prepare the macroporous hydroxyapatite scaffolds with interconnected oval shaped pores of 100–300 μm with pore wall thickness of ~50 μm. The compression strength of 60 wt.% HA loaded scaffold was 1.3 MPa. The biological response of the scaffold was investigated using human osteoblast like SaOS2 cells. The results showed that SaOS2 cells were able to adhere, proliferate and migrate into pores of scaffold. Furthermore, the cell viability was found to increase on porous scaffold compared to dense HA. The expression of alkaline phosphate, a differentiation marker for SaOS2 cells was enhanced as compared to nonporous HA disc with respect to number of days of culture. The enhanced cellular functionality and the ability to support osteoblast differentiation for porous scaffolds in comparison to dense HA has been explained in terms of higher protein absorption on porous scaffold.

Keywords: Hydroxyapatite; Compressive strength; Cell adhesion; ALP; Protein

1. Introduction

In the field of tissue engineering, it is well known that scaffolds, appropriately designed in terms of structure and properties play an important role [1–3] to direct and provide support to the growth of cells as well as their migration around surrounding tissue [4]. The majority of mammalian cell types are anchorage-dependent, meaning they will not be able to survive in the absence of an adhesion substrate. A number of experimental investigations suggest that the scaffolds with various compositions provide a suitable platform for cell attachment, proliferation, and cell migration [5]. As a consequence, efforts have been placed in the development of porous scaffolds for bone replacement and tissue engineering.

Hydroxyapatite [Ca_{10} $(PO_4)_6(OH)_2$], HA is one of the known biocompatible ceramic. HA has significant chemical and physical resemblance to the mineral constituents of human bones and teeth [6]. Being a bioactive ceramic, HA is widely used for various bone repairs and as coatings for metallic artificial device to improve their biological properties. HA has excellent biocompatibility, bioactivity and osteoconduction property. HA is thermodynamically the most stable calcium phosphate ceramic compound in solution, with the pH, temperature and composition nearest to that of the physiological fluid. In view of the above mentioned reasons, HA has a great ability of bond formation with the host tissue over most other bone substitutes, such as allograft or metallic implants.

In view of favorable property combinations as well as due to its close relationship with the mineral component of the bone and its excellent osteophilic properties [7,8], HA has been found as one of the materials of choice for the fabrication of inorganic scaffolds [9–11].

It is important to meet some criteria, while developing the porous scaffold to fulfill the requirements of the bone tissue engineering. The property requirements include, (a) it must be biocompatible, which enables the cell growth, their attachment to surface and proliferation, (b) the material should induce strong bone bonding, resulting in osteoconduction and osteoinduction, (c) rate of new tissue formation and biodegradability should match with each other, (d) the mechanical strength of the scaffolds should be adequate enough to provide mechanical constancy in load bearing sites prior to regeneration of new tissue and (e) porous structure and pore size of more than 100 μm for cell penetration, tissue in growth and

* Corresponding author. Tel.: +91 512 2597771; fax: +91 512 2597505.
E-mail address: bikram@iitk.ac.in (B. Basu).

0272-8842/$36.00
doi:10.1016/j.ceramint.2011.07.012

Table 1
Pore size distribution for an ideal scaffold in bone tissue engineering applications [12].

Pore size (μm)	Biological function
<1	Protein interaction, responsible for bioactivity
1–20	Cell attachment, their orientation of cellular growth (directionally)
100–1000	Cellular growth and bone ingrowth
>1000	Shape and functionality of implant

vascularisation (see also Table 1) [12]. As named, porosity is an important factor to allow cells to migrate via pores. The interconnected pores allow cells to migrate in multiple directions under real conditions.

In order to meet the required criteria for fabricating porous scaffold, several processing techniques have been employed. The most common techniques among all are gel casting [13], slip casting [14,15], fiber compacting [16], freeze casting [8] and gas foaming [17]. Gel casting is a wet ceramic forming technique, which involves the polymerization of a monomer in the presence of a solvent to form a rigid, ceramic-loaded body, which can be machined directly in a complex mold [18]. After gel formation, gel-cast green samples can be easily demolded and then are dried in controlled conditions [19]. Freeze casting is a method in which rapid freezing of a colloidal stable suspension of HA particles in a nonporous mold takes place, followed by sublimation of the frozen solvent under cold temperatures in vacuum.

Among these processes, polymer replication method offers the possibility of producing a tailored scaffold with controllable pore size using a polyurethane sponge as a template [20]. After considering limitations associated with various processes, the development of HA based porous scaffold in the present work is attempted using polymer replication method. The characteristics of the hydroxyapatite porous scaffolds and hydroxyapatite powder (starting material) were assessed by means of scanning electron microscopy (SEM), particle size distribution, X-ray diffraction (XRD), Fourier transformed infrared spectroscopy (FTIR) and compressive testing techniques. The in vitro biocompatibility properties were assessed using cell adhesion, MTT, ALP assay with SaOS2 cells and protein absorption study.

2. Experimental

2.1. Starting HA powders

Hydroxyapatite (HA) was synthesized by widely reported suspension–precipitation route, as described in our earlier work [21,22]. The precursor materials were CaO (M/s S.D Fine-Chem Lit., Product No. 37614), H_3PO_4 (M/s Merck, CAS No. 7664-38-2) and NH_4OH (M/s Qualikems, Product No. A025112). The particle size distribution was measured using laser particle size analyzer (Analysette 22, Fritsch GMBH, Germany).

2.2. Preparation of scaffold

The scaffolds were prepared using polymeric sponges infiltrated with ceramic slurry method that integrates the gel-casting and polymer sponge methods. The scaffolds were prepared using polyurethane sponges as a template. These polyurethane sponges were procured from commercial sources.

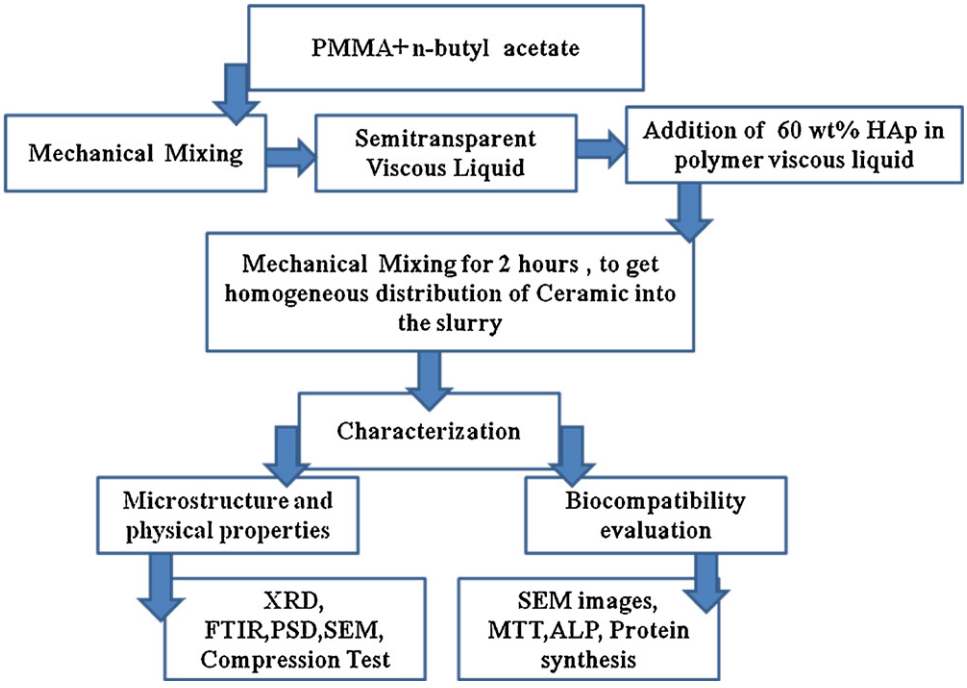

Fig. 1. Schematic illustration of preparation and characterization of porous scaffold.

The methodology, as shown in Fig. 1 was adopted for making the scaffold.

Several composition ratios were impregnated onto the polyurethane sponges and were analyzed. Finally, 60 wt.% HA loading was considered as the optimum, since the obtained scaffold has adequate strength to withstand manual handling. The polyurethane sponge was squeezed to remove excess slurry and treated from ambient according to the following sintering cycle: heating at 2 °C/min from ambient to 600 °C followed by a 1 h plateau; heating at 3 °C/min from 600 °C followed by another plateau of 1 h. Then, the furnace power was turned off and the samples were allowed to cool inside the furnace for 24 h. For comparison, HA powder were compacted and pressureless sintered at 1200 °C for 1 h to obtain nonporous dense HA (density-98.5% ρ_{th}).

2.3. Characterization of prepared scaffold

XRD analysis was carried out to identify different phases present in the starting powders as well as in the as-sintered scaffold. The phases of the prepared scaffolds were determined using CuKα radiation over the 2θ range of 5–70° with a step size of 0.05°. In order to analyze the scaffolds, the scaffold was reduced to powder. The phase dissociation behavior of HA or formation of any reaction product was studied by analyzing XRD data.

The particle size distribution of as synthesized HAp powder and compressed scaffold powder (after compression test) was measured using laser particle size analyzer (Analysette 22, Fritsch GMBH, Germany).

Fourier Transform Infrared Analysis (FT-IR, vortex 70, BRUKER) was carried out using ball milled powders in the range of 400–4000 cm^{-1} to obtain information about the various chemical bonds.

A liquid displacement method was used to measure the porosity and density of 60 wt.% HA scaffolds [23].

The mechanical properties were calculated from stress vs. strain curve using the mechanical testing machine, INSTRON 1195. The samples used for the compression test were of rectangular shape and were tested with crosshead speed of 0.5 mm/min using the load cell of 1 KN. Microstructural investigation of the scaffold was performed by means of SEM (FEI-SEM, model JSM-6330F, Philips, The Netherlands). Prior to SEM observation, the samples were sputter-coated with a thin Au-Pd coating in order to obtain sufficient conductivity on the surface and to avoid charging of the surface in the SEM.

2.4. In vitro biocompatibility properties

2.4.1. Cell culture experiments

Human osteoblast SaOS2 cell lines were procured from ATCC, USA. Prior to seeding the cells on scaffold, the cells were revived. SaOS2 cells were cultured in McCoy's medium 5A (Sigma–Aldrich), supplemented with 15% FBS and 1% penicillin/streptomycin solution. Cells were cultured at 37 °C in humidified air with 5% CO_2 until confluent. The medium was being replaced time to time to control the pH. The numbers of cells in confluent monolayer were approximately 5×10^5/ml. The confluent monolayer was detached from the tissue culture flask using 0.5% trypsin, and 0.2% EDTA solution (Sigma–Aldrich).

2.4.2. Cell adhesion test

Before cell seeding, the scaffolds were ultrasonically cleaned and then dehydrated with 70% ethanol for 24 h to sterilize [24]. Ethanol was removed by washing the scaffolds three times with phosphate-buffer saline (PBS) for 1 h. The scaffolds were then exposed to UV light for 2 h, and finally soaked in medium containing 10% fetal bovine serum (FBS) for 12 h.

As described in the previous subsection, SaOS2 cells were grown and then subcultured. After subculturing, the cells were washed with phosphate buffer saline (PBS, synthesized in our laboratory), detached with trypsin solution at 37 °C for 5 min and counted using haemocytometer. Then, the cells were seeded on the dense HA, porous scaffold and control plastic disc at approximate density of 5×10^5/ml. The culture plates (4 well) along with test samples were then incubated in a CO_2 incubator with the previously described environment. The culture medium was being aspirated time to time and fresh culture medium was being added to the culture plate wells. After the stipulated time period (7 and 10 days), the samples were washed twice with phosphate buffer saline (PBS) and then, cells were fixed with 1.5% glutaraldehyde diluted in PBS. The cells, adhered on the material surfaces, were dehydrated using a series of ethanol solution (30, 50, 70, 90 and 100%) for 10 min twice and then further dried using hexa methyl di silazane (HMDS). The dried samples were sputter coated (Vacuum Tech, Bangalore, India) with gold and examined under scanning electron microscope (SEM: Philips, Quanta).

2.4.3. MTT assay

Mitochondrial dehydrogenase activity of the SaOS2 cell was determined using a biochemical 3(4,5-dimethylthiazol-2yl)-2-5 diphenyltetrazolium bromide, SIGMA, USA), which was reduced to formazan that accumulated in the cytoplasm of the viable cells. For this purpose, the sterile scaffold along with control and dense HA were placed in the 24 well plate (exposed in UV for 30 min) and cells were seeded (200 μl DMEM with cell suspension, serum and antibiotic) approximately at a density of 3×10^5/ml. Subsequently, the culture plate having replicates of each composition was incubated for 3, 5 and 7 days in CO_2 incubator. After the required incubation period, 10 μl of reconstitute MTT was added in each well (5 mg/ml in DMEM without Phenol red and serum) and plate was incubated for 6–8 h. After the formation of formazan crystal, the samples were removed from the well and 100 μl of DMSO (stock solution) was added in each well, including control. The absorbance was measured at 540 nm using ELISA automated microplate reader (Bio-Tek, ELx800).

2.4.4. Alkaline phosphate activity (ALP) assay

ALP assay is used to assess osteoblast differentiation. In this study, the ALP activity was measured using a commercial kit (N2770, Fast PNPP, Sigma Aldrich). Briefly, the osteoblast cells were seeded on scaffolds in 24 well plates. HA disc was used as control. The osteoblast cells were harvested on dense

HA and porous scaffold for 3, 5 and 7 days. At the end of each interval, each specimen was incubated with addition of 100 μl of a p-nitrophenyl phosphate solution at 37 °C for 30 min. The production of p-nitrophenol in the presence of ALP was measured by monitoring light absorbance by solution at 405 nm using ELISA reader. The process was repeated for 3 times for each time scale per sample.

2.4.5. Protein absorption

The BCA Protein Assay is the combination of very well-known reduction process. In this process, reduction of Cu^{2+} to Cu^{1+} takes place by protein in an alkaline medium with detection of the cuprous cation (Cu^{1+}) by bicinchoninic acid (BCA). The intensity of the color produced is proportional to the number of peptide bonds participating in the reaction. BCA is a highly sensitive colorimetric detection reagent, which reacts with the cuprous cation (Cu^{1+}) [25]. The purple-colored reaction product is formed by the chelation of two molecules of BCA with one cuprous ion. The purple color may be measured at any wavelength between 540 nm and 570 nm with minimal (less than 10%) loss of signal.

The protein adsorption study in the present case was performed using bovine serum albumin (BSA), following standard protein adsorption protocol. The equal protein source was filled in 24 well plate containing sterile scaffold samples. The plate was then placed in a sterile incubator at 37 °C for standard incubation time. The samples were then washed with equal volume of DI water to remove the non-adherent proteins. Then all the samples were washed with equal amount of 1 × PBS to get the absorbed protein dissolved. Thereafter, 1 × PBS was then placed in another well plate. 1% Sodium docedyl sulfate (SDS) solution was added to each well containing sample and incubated at 50 °C for 15 min. Protein concentration was finally analyzed using the bicinchronic acid (BCA) protein assay.

2.5. Statistical analysis

MTT and ALP results were statistically analyzed using the commercial SPSS-13.0 software. To measure the statistical difference among absorbance values, we use the analysis of variance (ANOVA) method. In particular, the post hoc

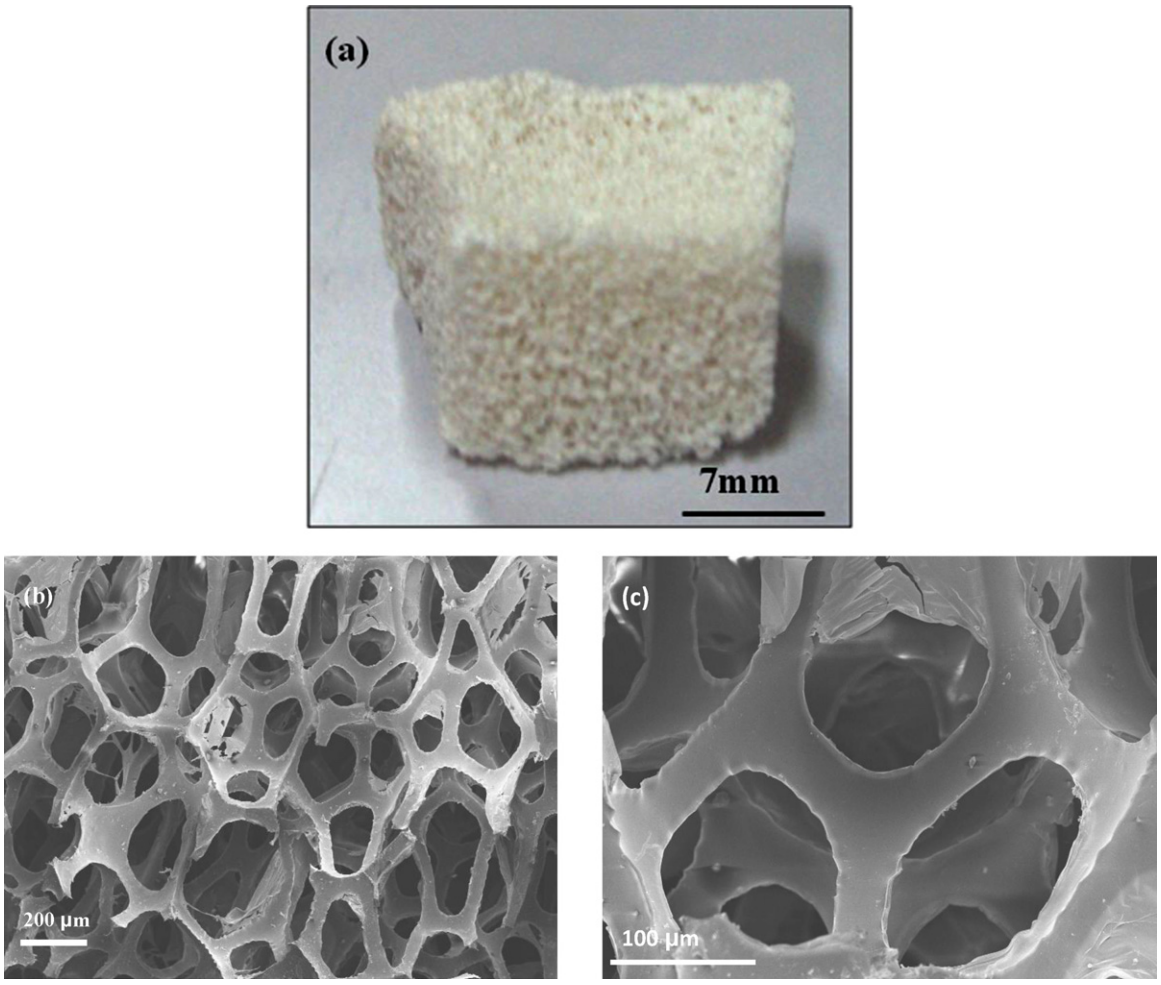

Fig. 2. (a) Porous hydroxyapatite body of rectangular shape produced via. Polymeric sponge method using sol–gel derived HA powder and polymer slurry (b) and (c) SEM of scaffold.

comparison of the mean of independent groups was made using Tukey test at statistical significance value of $p < 0.05$.

3. Results and discussion

3.1. Microstructure and physical properties

Fig. 2a represents the micrograph of as synthesized porous HA scaffold. It is seen that there is no sharp faceted geometrical shape. The polymer replication method was useful to produce HA scaffolds of cube like shape or with rectangular cross-section. The largest scaffold was of 25 mm × 25 mm × 25 mm dimension. Another important aspect is that this synthesis route to prepare scaffold provides better strength to handle with better reproducibility. The pore size was ranging between 100 μm and 300 μm (Fig. 1b) and the pore wall thickness was measured as 50 μm (see Fig. 1c). Most of the pores are oval shaped and uniformly distributed.

It can be mentioned here that the scaffolds are required to reproduce the bone characteristics not only in terms of composition, but also in terms of pore morphology. Porous implants allow development of bone and soft tissues within large pores and also blood supply for further bone mineralization. Based on the presence of open pores, porosity can be characterized in relation to properties like permeability and surface area of the porous structure. High porosity can be correlated with high surface area to volume ratio, and thus favors cell adhesion to the scaffold and promotes bone tissue regeneration.

Fig. 3 plots the X-ray diffraction patterns of the hydroxyapatite scaffolds. No new phase (after sintering) is formed and all peaks correspond solely to hydroxyapatite phase. Moreover, the peaks were sharp and distinct, which indicated that porous scaffold were highly crystalline. Also, the sintering at 1200 °C does not cause any dissociation of HA to TCP.

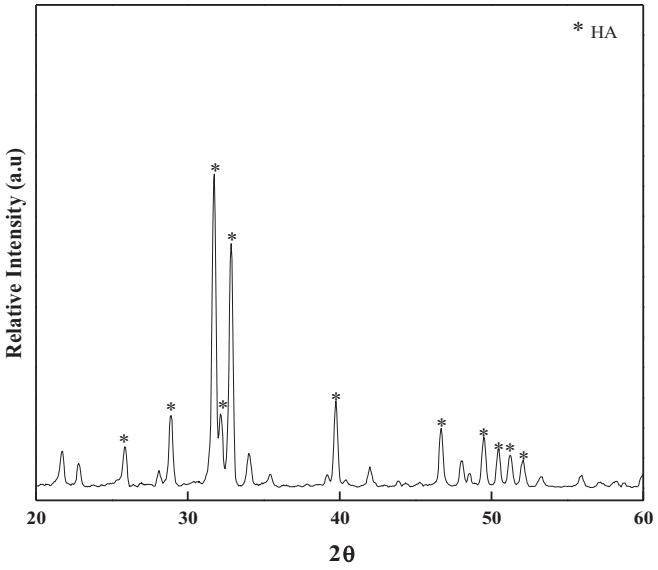

Fig. 3. XRD spectrum of prepared scaffold after compression test obtained by polymer replication method.

In the IR spectra (Fig. 4), two FT-IR bands at 635 and 3568 cm^{-1} correspond to the vibration of hydroxyl ions (OH^-). The ones at 1030 and 565 cm^{-1} are the characteristic bands of phosphate (PO_4^{3-}) bending vibration, while the band at 985 cm^{-1} is attributed to phosphate stretching vibration. The

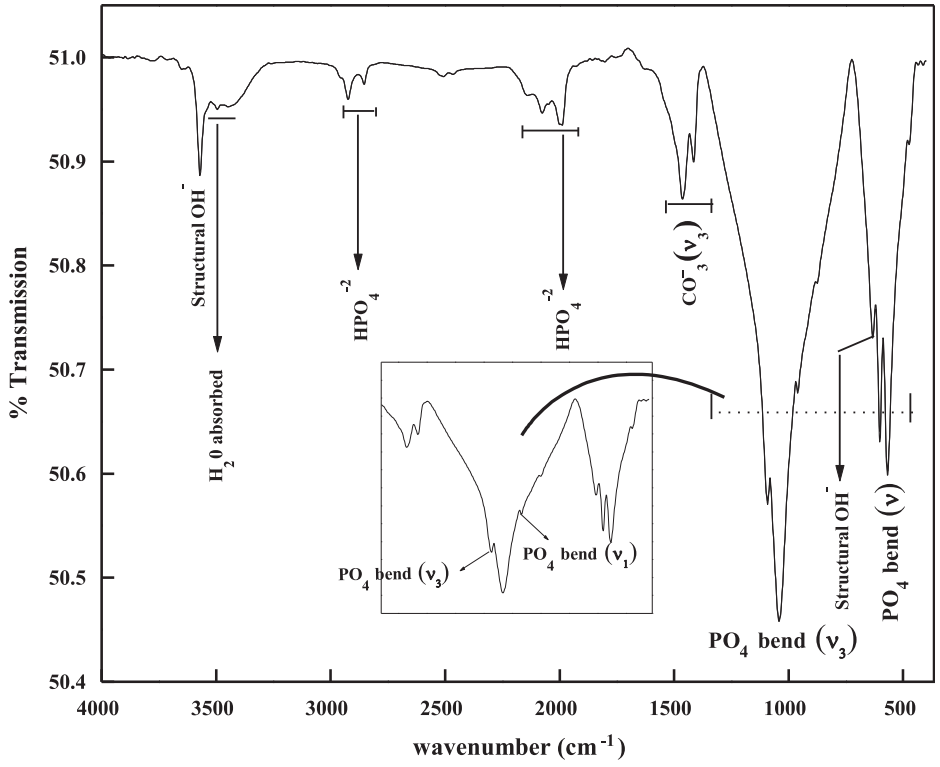

Fig. 4. Fourier transform infrared (FTIR) spectrum of the sintered hydroxyapatite sponge.

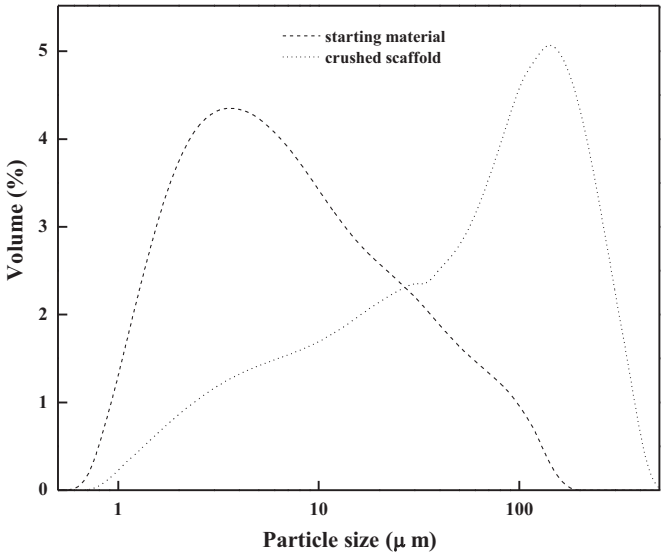

Fig. 5. Particle size distribution of the HA powder (starting material) and crushed scaffold obtained by replication method.

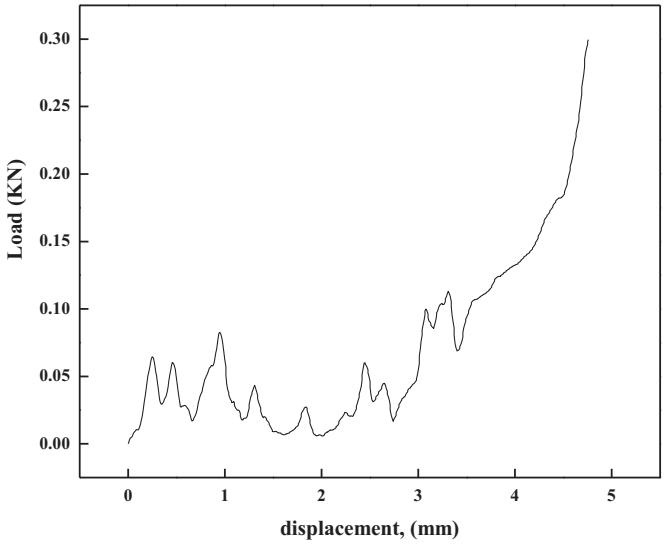

Fig. 6. Compressive load/displacement curve of the prepared porous scaffold.

bands at 886, 1410 and 1465 cm^{-1} are indicative of the carbonate ion (CO_3^{2-}) substitution. The bands at 1650 and 3450 cm^{-1} correspond to H_2O absorption. The analyses of these bands confirmed that the FTIR spectra recorded with porous scaffold correspond to HA [26,27].

There is a clear OH^- peak at 3450 cm^{-1}, followed by some broad peaks between 2918 cm^{-1} and 2850 cm^{-1}, may correspond to HPO_4^{2-} groups as previously reported in the literature [28]. Phosphate bands υ_3 were identified by two peaks at 1102 and 1033 cm^{-1}, whereas the υ_1 shoulder band is present at 965 cm^{-1}. The shoulder bands with lower intensity located between 1990 cm^{-1} and 2112 cm^{-1} may correspond to HPO_4^{2-} groups, as previously reported elsewhere [18]. Furthermore, the phosphate υ_2 band was also observed at 468 cm^{-1} being followed by phosphate υ_4 bands at peaks 603 and 550 cm^{-1}, respectively. There was no discernible spectrum difference between the HA powder and HA scaffold, which further confirms that no chemical decomposition occurred during the sintering process.

The particle size distribution of the crushed hydroxyapatite powder and as synthesized porous scaffold are shown in Fig. 5. The hydroxyapatite powder presents a mono-modal distribution with an average particle size of 6.5 μm, whereas the crushed hydroxyapatite scaffolds present a blunt bimodal distribution with two maxima at ∼6.5 and ∼61 μm. The hydroxyapatite powders have larger specific surface area than that of the hydroxyapatite porous scaffolds, presenting values of 1.38 m^2/g and 0.47 m^2/g, respectively. It is evident that high porosity usually attributes high surface area to volume ratio, which should favor cell adhesion and encourages bone tissue regeneration.

The pore architecture of scaffold directly affects its mechanical strength [29]. Since a higher density usually leads to higher mechanical strength, high porosity provides a favorable biological environment. Therefore, a balance between the porosity and density for a scaffold must be established for the specific application. The measured apparent density and porosity of HA scaffolds prepared with slurries of different HA concentrations using the method shown before (Fig. 2) were 0.74 g cm^3 and about 70%, respectively. The apparent density of trabecular bone ranges from 0.14 g cm^3 to 1.10 g cm^3 (average: 0.62 ± 0.11 g cm^3) [30].

The compressive strength was determined from stress–strain curve by applying load until scaffold was crushed. A typical compressive stress/displacement curve of the porous samples is provided in Fig. 6. The mechanical response shows an early abrupt descent, with stress values increasing until a maximum was reached. It is evident that, as the test progressed, pores started to be crushed. Eventually, the sample densification occurred and due to this phenomenon, some of the tested samples did not even break. The mechanical properties of a porous material depend on the density of the porewall material [31]. It can be easily explained by the simple mechanism of pore filling [32]. Initially, when the load was applied, the initial layer was compressed and covers the pores of next layer and become denser compared to unloaded scaffold. The compressed particles in agglomerate fill the void space and increase the density. Such behavior is reflected in stress vs. strain curve (Fig. 6). At the starting point, the plot is not smooth, but after getting dense body, the mechanical response becomes smooth up to maximum load point.

The maximum compressive strength for the prepared scaffold was determined as 1.3 MPa, which resembles with earlier reported data as well as close to strength of natural bone [33]. The compressive strength of porous human bone ranges between 2–12 MPa for cancellous bone and 100–230 MPa for cortical bone [34]. On the other hand, the mechanical strength of porous HA is reported in the range of 1.2–16 MPa [35]. The compressive strength of porous HA after implantation of 3 months is reported as 2–20 MPa [36].

3.2. Biocompatibility evaluation

The biological performance of porous HA-scaffold was evaluated using SaOS2 osteoblast like cells. SEM results

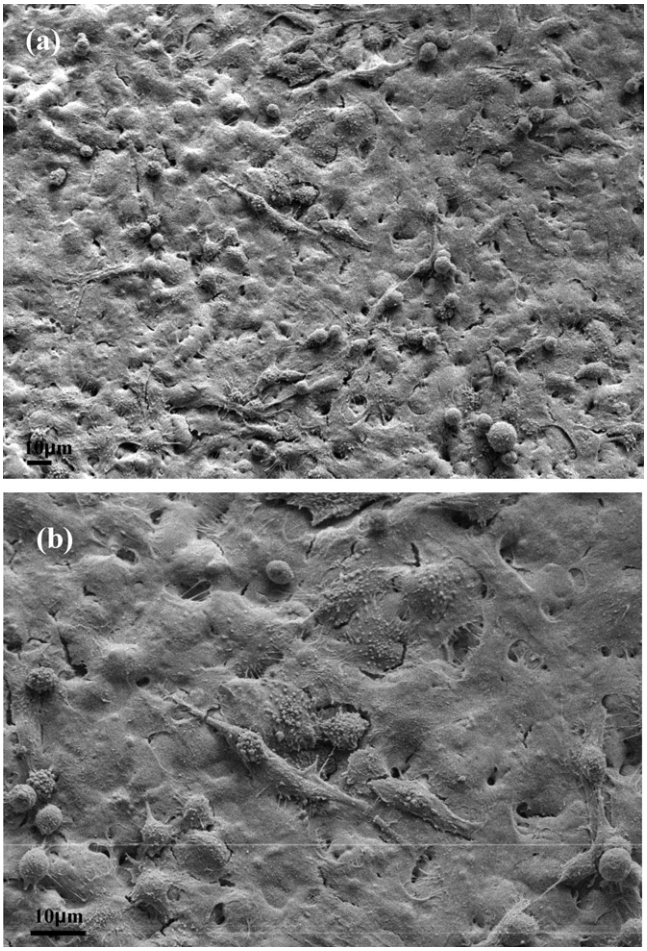

Fig. 7. SEM image of osteoblast cells cultured on scaffold (a) after 7 day and (b) after 10 day of culture.

indicated that the scaffold allowed the attachment and spreading of the cells, while keeping a normal cellular morphology. As shown in Fig. 7, the cells are well attached and spread on the scaffold, presenting a round shaped configuration with extended filapodia in multiple directions, adhering to the scaffold surface. After 7 days of culture, cells showed a typical morphology presenting a well spread configuration with more lamellopodia connecting to neighboring cells, starting to form a continuous cell layer. After 10 days of incubation, virtually the entire surface was covered by cells, and in some cases, continuous sheet of cell was seen. Similar behavior was previously observed by Bagamsia and Joos [37].

The results of MTT assay (Fig. 8) demonstrate that the scaffold along with dense HA, stimulated the proliferation of osteoblast cells to a similar extent with similar difference in OD values after 3/5/7 days of incubation. Independent of incubation period, the porous scaffolds exhibited better cell viability in comparison to dense HA. Such observations show efficacy of the porous scaffold. The pore walls provide good space for cells to proliferate in denser way. The post hoc multiple comparison among the samples revealed that the scaffold showed the significant difference with sintered HA. The viability of the SaOS2 cells was found to be superior in case of scaffold than

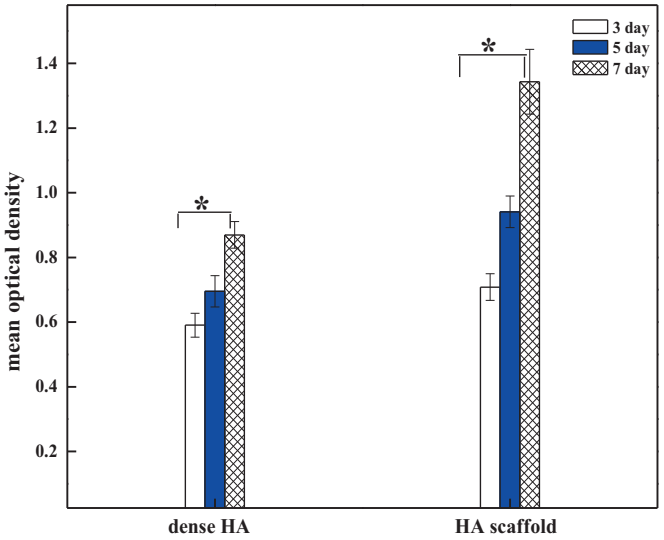

Fig. 8. MTT assay results showing the SaOS2 cells on HA and porous scaffold after 3, 5 and 7 days of culture. *Represent significant difference at $p < 0.05$ with respect to compositions and Error bars correspond to ±1.00 SE for number of days of culture.

that of cells cultured on sintered HA. In summary, it can be said that the scaffold shows good cytocompatibility as well as enhanced cell viability property with respect to incubation period.

ALP is a representative enzyme of osteoblastic differentiation, and ALP activity is considered as an indicator of osteoblastic differentiation of SaOS2 cells cultured on the scaffolds. As shown in Fig. 9, ALP expression of cells grown on sintered HA and HA scaffold increased continuously over the varying culture duration. After day 3, the ALP activity on the scaffolds was low, and then increased on day 5 and 7. The ALP

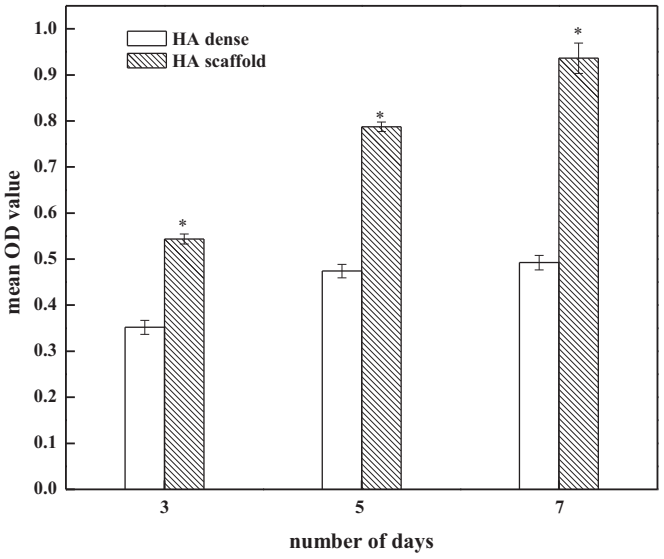

Fig. 9. ALP assay results showing the SaOS2 cells on control, HA and Hybrid composite samples after 3, 5 and 7 days of culture. *Represent significant difference at $p < 0.05$ with respect to compositions and Error bars correspond to ±1.00 SE for number of days of culture.

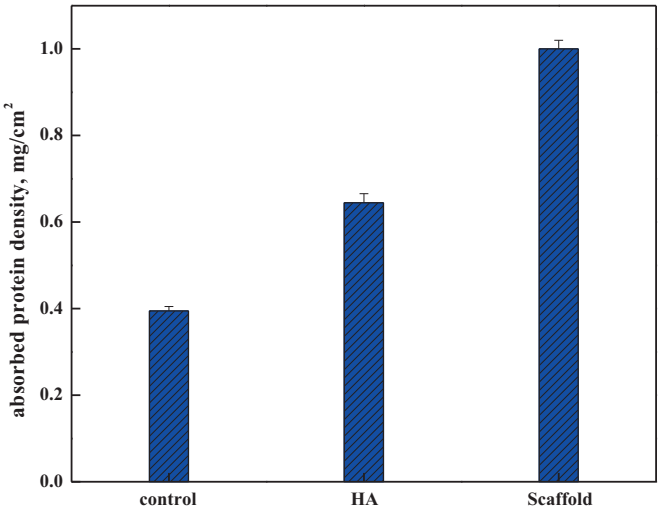

Fig. 10. Comparison of BSA protein absorption behavior of scaffold with dense HA and negative control disc after incubation for 4 h.

activity of osteoblast-like cells grown on the porous scaffolds for various culture times was significantly higher than that of dense HA.

The cellular functionality in terms of adhesion, proliferation and differentiation depends on protein adsorption on scaffold, which is a necessary biological pre-requisite process.

As explained in Section 2.4.5, the rate of BCA color formation is dependent on the incubation temperature, the type of protein and the relative amounts of reactive amino acids contained in the proteins. Fig. 10 presents the absorbed protein density on control disc, dense HA and porous scaffold after 4 h incubation. It is clearly evident that the protein density is approximately 4 fold of control disc and approximate 2 fold of dense HA after 4 h of incubation period. These results corroborate well with cell adhesion and viability assay, as the cell adhesion is directly related to the amount of protein absorbed on the surface.

In summary, it can be stated that the pore size distribution and surface chemistry provided favorable topographical substratum for cell attachment and ingrowth in the present case. In particular, the scaffold surface favored enhanced surface wetting properties, which could affect cell attachment directly or indirectly through selective adsorption of serum protein required for cell attachment. It is known that the absorbed protein modulated cellular interactions [38].

It is also well known, that the physicochemical features of the ceramic surface can affect the reorganization of proteins on porous scaffold and change the profile of absorbed proteins [39]. The pore wall thickness and homogeneous distribution of oval shaped pores provided larger surface area to facilitate protein absorption and cell proliferation as well as cell viability and osteoblast differentiation.

4. Conclusions

a) The present investigation confirms, that it is possible to produce porous scaffold with homogeneous pore distribution and pore wall thickness using polymer sponge replication method. While the pore size varies between 100 μm and 300 μm, the pore wall thickness was ∼50 μm. The apparent density and porosity of HA scaffold were calculated of 0.74 g cm^3 and ∼70%, respectively.
b) The compressive strength of porous scaffold was calculated as 1.3 MPa, which correlates well with the strength of natural cancellous bone.
c) The HA based porous scaffold could support the attachment, growth and ALP production of human osteoblast type SaOS2 cells. The experimental results revealed that porous scaffold could provided better substrate for cell adhesion and proliferation and differentiation of osteoblast type cells, in comparison to dense sintered HA. Such difference has been explained in terms of higher protein absorption on porous scaffold.

Acknowledgments

This project was partially supported by Department of Science and Technology, New Delhi, India, under Fast Track Young Scientist Scheme. The cell culture facility was established with the funding from Department of biotechnology, Government of India.

References

[1] G.P. Dillon, X. Yu, A. Sridharan, J.P. Ranieri, R.V. Bellamkonda, The influence of physical structure and charge on neurite extension in a 3D hydrogel scaffold, J. Biomater. Sci. Polym. Ed. 9 (1998) 1049–1069.
[2] L.M.Y. Yu, N.D. Leipzig, M.S. Shoichet, Promoting neuron adhesion and growth—review, Mater. Today 11 (2008) 36–43.
[3] S.H. Bhang, J.S. Lim, C.Y. Choi, Y.K. Kwon, B.S. Kim, The behaviour of neural stem cells on biodegradable synthetic polymers, J. Biomater. Sci. Polymer. Ed. 18 (2007) 223–239.
[4] E.H. Groeneveld, J.P. Van den Bergh, P. Holzmann, C.M. Ten Bruggenkate, D.B. Tuinzing, E.H. Burger, Mineralization processes in de-mineralized bone matrix grafts in human maxillary sinus floor elevations, J. Biomed. Mater. Res. 48 (1999) 393–402.
[5] C.A. Leony Leon, New perspectives in mercury porosimetry, Adv. Colloid Interface Sci. 76–77 (1998) 341–372.
[6] K. Shigeru, T. Oku, S. Takagi, Hydraulic property of hydoxyapatite thermal decomposition product and its application as a biomaterial, J. Ceram. Soc. Jpn. Int. Ed. 97 (1989) 96–101.
[7] J. Cesarano III, J.G. Dellinger, M.P. Saavedra, D.D. Gill, R.D. Jamison, B.A. Grosser, J.M. Sinn-Hanlon, M.S. Goldwasser, Customization of load-bearing hydroxyapatite lattice scaffolds, Int. J. Appl. Ceram. Technol. 2 (2005) 212–220.
[8] S. Lenhert, M.B. Meier, U. Meyer, L. Chi, H.P. Wiesmann, Osteoblast alignment, elongation and migration on grooved polystyrene surfaces patterned by Langmuir–Blodgett lithography, Biomaterials 26 (2005) 563–570.
[9] B.S Chang, C.K. Lee, K.S. Hong, H.J. Youn, H.S. Ryu, S.S. Chung, K.W. Park, Osteoconduction at porous hydroxyapatite with various pore configurations, Biomaterials 21 (2000) 1291–1298.
[10] R.M. Pilliar, M.J. Filiaggi, J.D. Wells, M.D. Grynpas, R.A. Kandel, Porous calcium polyphosphate scaffolds for bone substitute applications-in vitro characterization, Biomaterials 22 (2001) 963–972.
[11] E.C. Shors, R.E. Holmes, in: L.L. Hench, J. Wilson (Eds.), An Introduction to Bioceramics, World Scientific, NJ, 1993, p. 181.
[12] S. Sálcedo S, D. Arcos, M. Vallet-Regí, Upgrading calcium phosphate scaffolds for tissue engineering applications, Key Eng. Mater. 377 (2008) 19–42.

[13] P. Sepulveda, F. Ortega, M.D.M. Innocentini, V.C. Pandolfelli, Properties of highly porous hydroxyapatite obtained by the gelcasting of foams, J. Am. Ceram. Soc. 83 (2001) 3021–3024.
[14] L.A. Cyster, D.M. Grant, S.M. Howdle, F. Rose, D.J. Irvine, D. Freeman, et al., The influence of dispersant concentration on the pore morphology of hydroxyapatite ceramics for bone tissue engineering, Biomaterials 26 (2005) 697–702.
[15] Q. Fu, M.N. Rahaman, B.S. Bal, W. Huang, D.E. Day, Preparation and bioactive characteristics of a porous 13-93 glass and fabrication into the articulating surface of a proximal tibia, J. Biomed. Mater. Res. A 82 (2007) 222–229.
[16] B.S. Chang, C.K. Lee, K.S. Hong, H.J. Youn, H.S. Ryu, S.S. Chung, et al., Osteoconduction at porous hydroxyapatite with various pore configurations, Biomaterials 21 (2000) 1291–1298.
[17] L.D. Harris, B.S. Kim, D.J. Mooney, Open pore biodegradable matrices formed with gas foaming, J. Biomed. Mater. Res. 42 (1998) 396–402.
[18] A.C. Young, O.O. Omatete, M.A. Janney, P.A. Menchhofer, Gelcasting of alumina, J. Am. Ceram. Soc. 74 (1991) 612–618.
[19] S.D. Nunn, G.H. Kirby, Green machining of gelcast ceramic materials, Ceram. Eng. Sci. Proc. 17 (1996) 209–213.
[20] A.C. Queiroz, S. Teixeira, J.D. Santos, F.J. Monteiro, Production of porous hydroxyapatite with potential for controlled drug delivery, Adv. Mater. Forum Ii 455 (2004) 358–360.
[21] S. Nath, A. Dey, A.K. Mukhopadhyay, B. Basu, Nanoindentation response of novel hydroxyapatite–mullite composites, Mater. Sci. Eng. A 513–514 (2009) 197–201.
[22] S. Bodhak, S. Nath, B. Basu, Friction and wear properties of novel HDPE–HAp–Al_2O_3 composites against alumina counterface, J. Biomater. Appl. 23 (2009) 407–433.
[23] R. Hodgkinson, J.D. Curry, Effect of variation in structure on Young's modulus of cancellous bone. A comparison of human and non human material, Proc. Inst. Mech. Eng. [H] 204 (2002) 115–121.
[24] A.G. Mikos, M.D. Lyman, L.E. Freed, R. Langer, Wetting of poly(L-lactic acid) and poly(DL-lactic-co-glycolic acid) foams for tissue culture, Biomaterials 15 (1994) 55–58.
[25] www.biotek.lu.se/fileadmin/bioteknik/../KBT050_LabManual-10.pdf.
[26] F. Chen, Z.C. Wang, C.J. Lin, Preparation and characterization of nano-sized hydroxyapatite particles and hydroxyapatite/chitosan nano-composite for use in biomedical materials, Mater. Lett. 57 (2002) 858–861.
[27] R.N. Panda, M.F. Hsieh, R.J. Chung, T.S. Chin, FTIR, XRD, SEM and solid state NMR investigations of carbonate-containing hydroxyapatite nano-particles synthesized by hydroxide-gel technique, J. Phys. Chem. Solids 64 (2003) 193–199.
[28] I.R. Gibson, S.M. Best, W. Bonfield, Chemical characterization of silicon-substituted hydroxyapatite, J. Biomed. Mater. Res. 44 (1999) 422–428.
[29] P. Sepulveda, F.S. Ortega, M.D.M. Innocentini, V.C. Pandolfelli, Properties of highly porous hydroxyapatite obtained by the gelcasting of foams, J. Am. Ceram. Soc. 83 (2000) 3021–3024.
[30] L.A. Evans, D.J. Macey, J. Webb, Calcium biomineralization in the regular teeth of the chiton, acanthopleura hirtosa, Calcified Tissue Int. 51 (1992) 78–82.
[31] L.J. Gibson, M.F. Ashby, Cellular Solids, Structure and Properties, Cambridge Solid State Science Series, second ed., Cambridge University Press, Cambridge, UK, 1997, pp. 429–452.
[32] Q.Z Chen, I.D. Thompson, A.R. Boccaccini, 5S5 Bioglass®-derived glass–ceramic scaffolds for bone tissue engineering, Biomaterials 27 (2006) 2414–2425.
[33] Y. Zhang, M. Zhang, Three dimensional macroporous calcium phosphate bioceramics with nested chitosan sponges for load bearing implants, J. Biomed. Mater. Res. 61 (2002) 1–8.
[34] L.L. Hench, J. Wilson, in: L.L. Hench, J. Wilson (Eds.), An Introduction to Bioceramics, World Scientific, Singapore, 1993, pp. 12–26.
[35] H. Yoshikawa, A. Myoui, Bone tissue engineering with porous hydroxyapatite ceramics, J. Artif. Organs 8 (2005) 131–136.
[36] I. Sopyan, N.S. Sulaiman, D. Gustiono, N. Herdianto, Porous hydroxyapatite-gelatin composites with functions of bone substitutes and drug releasing agents: a preliminary study, BioMEMS and Nanotechnology II, SPIE, Int. Soc. Opt. Eng. 6036 (2006) C1–C11.
[37] F.B. Bagambisa, U. Joos, Preliminary studies on the phenomenological behavior of osteoblasts cultured on hydroxyapatite ceramics, Biomaterials 11 (1990) 50–56.
[38] H. Zeng, K.K. Chittur, W.R. Lacefield, Analysis of bovine serum albumin adsorption on calcium phosphate and titanium surfaces, Biomaterials 20 (1999) 377–384.
[39] A. Laczka-Osyczka, M. Laczka, S. Kasugai, K. Ohya, Behavior of bone marrow cells cultured on three different coatings of gel-derived bioactive glass-ceramics at early stages of cell differentiation, J. Biomed. Mater. Res. 42 (1998) 433–442.